*Transactions*, SMiRT-25
Charlotte, NC, USA, August 4-9, 2019
Division V

# SEISMIC RESPONSE OF ROCKING FRAMES WITH UNSYMMETRICAL PIERS

**Amitabh Dar[1], Dimitrios Konstantinidis[2], and Wael W. El-Dakhakhani[3]**

[1] Technical Advisor, Bruce Power, Canada. Doctoral Researcher, McMaster University, Hamilton, ON, L8S 4L7, Canada (dara@mcmaster.ca)
[2] Assistant Professor, Civil & Environmental Engineering, University of California, Berkeley, USA.
[3] Professor and University Scholar, Department of Civil Engineering and the School of Computational Science & Engineering, McMaster University, Hamilton, ON, L8S 4L7, Canada

## ABSTRACT

The seismic response of rocking frames consisting of a rigid beam freely supported by vertically symmetrical rigid piers has been studied in recent literature. When these types of frames engage in rocking motion, the piers experience equal rotations, and the top beam undergoes translation but no rotation. The frame's seismic response has been shown to be influenced by the top support eccentricity, which is defined as the distance of the beam-to-pier contact edge to the pier's vertical axis of symmetry. Such a frame can be represented by a dynamically equivalent rocking block. Some rocking frames in nuclear power plants, however, consist of piers that are vertically unsymmetrical and undergo unequal rotations during rocking motion, with the top rigid beam experiencing both translation and rotation. In this case, it is observed the dynamic parameters of an equivalent block vary because of their dependence on the instantaneous rotations of the piers and the top beam, which change during rocking motion. Thus, a time-independent dynamically equivalent rocking block for a frame on unsymmetrical piers does not generally exist. However, it is possible to engineer the top support eccentricities so that even though the piers are unsymmetrical, they experience equal rotations during rocking motion, and the top beam translates without rotating, leading to time-independent parameters of a rocking block. This paper presents expressions for the parameters of an equivalent block for rocking frames with unsymmetrical piers. Response history analysis of these systems is carried out to investigate their behavior under select earthquake motions.

## INTRODUCTION

In a nuclear power plant (NPP) seismic interaction of an unanchored component with a safety-related system or component poses risk to nuclear safety. To avoid rocking and sliding caused by a seismic event, the ASCE 43-05 (2005) standard recommends anchoring of components. However, it does allow unanchored components provided that the requirements of the standard for estimating the rocking or sliding response and providing sufficient clearance around the component are satisfied. The standard outlines an approximate method to obtain the pure planar rocking response of an unanchored slender component based on the premise that a rocking block can be considered as an equivalent single-degree-of-freedom (SDOF) viscously damped linear oscillator. Dar et al. (2016a) demonstrated this method to be unreliable and confirmed that a rocking object cannot be represented by a SDOF oscillator as concluded by Makris and Konstantinidis (2003). Priestley et al. (1978) and Wesley et al. (1980) also attempted to estimate the rocking response of a rigid block by considering it to be equivalent to a SDOF oscillator. The methodology by Priestley et al. (1978) was found to be erroneous by Makris and Konstantinidis (2003) who introduced the novel concept of *rocking spectrum* that can readily provide the peak rocking response

of a rigid block to a seismic event. The methodology given by Wesley et al. (1980) was evaluated by Dar et al. (2013) in a preliminary study demonstrating that it leads to inaccurate results.

On several occasions, rocking response of assemblages of rigid unanchored components is required to be computed. However, if such an assemblage can be represented by a dynamically equivalent rocking block having the same response as the assemblage, its response can be obtained from a rocking spectrum (Makris and Konstantinidis, 2003). Stacked-block assemblages have been studied by several authors, including Lee (1975), Ikushima and Nakazawa (1979), Psysharis (1990), Spanos et al. (2001), Konstantinidis and Makris (2005), Kounadis et al. (2012) and Minafo et al. (2016), and references therein. The seismic response of asymmetric rocking single-body structures and dual-body systems was estimated by Wittich and Hutchinson (2015, 2017) through extensive shake table test studies.

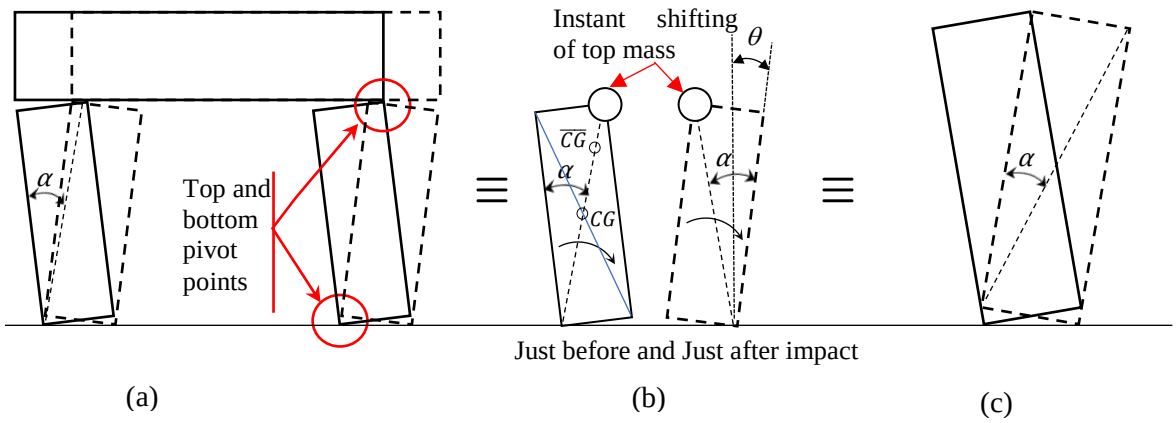


Figure 1: Rocking frame: (a) dashed and solid lines show the convention for positive and negative rotations, respectively (pivot points shown for negative rotation) (b) equivalent assembly of block with top lumped mass under positive and negative rotation, and (c) dynamically equivalent rocking block

Parameters of solitary blocks dynamically equivalent to various types of assemblages other than the stacked blocks were studied by DeJong and Dimitrakopoulos (2014). Dimitrakopoulos and Giouvanidis (2015) studied rocking frames with top beam rotation but without the effect of top-eccentricity. Figure 1(a) shows a rocking frame studied by Makris and Vassiliou (2013), where the top beam is in contact with the top right corners of the piers when in rocking motion from right to left (counterclockwise rotation) and vice versa for the motion from left to right. Sufficient friction is assumed at all contact points to prevent sliding. In this frame, the top rigid beam maintains point contacts with the top corners of the piers. Since the distances of the top contact points from their respective pivots, i.e., the pier diagonals, are equal, the piers experience the same rotation, and the top beam remains horizontal. Parameters of a dynamically equivalent rocking block, shown in Figure 1(c) were established by Makris and Vassiliou (2013), concluding that an equivalent block has the same slenderness, represented by parameter $\alpha$, as that of a solitary pier but is bigger in size. This was investigated further by Dar et al. (2015, 2016b, 2018) who demonstrated that the entire frame can be represented by a pier with a top lumped mass, equal to the tributary mass of the beam, as shown in Figure 1(b). Since the center of gravity of such an assembly ($\overline{CG}$) remains on the pier diagonal, there is no change in its slenderness compared to the center of gravity of a solitary pier ($CG$). However, since $\overline{CG}$ is higher than $CG$ of the solitary pier, its effective size is bigger. Upon impact, the top lumped mass shifts instantly from one pier corner to the other, and hence, $\overline{CG}$ remains along the pier diagonal. Due to the size effect noted first by Housner (1963), whereby the bigger of two geometrically similar blocks experiences smaller rotation, Makris and Vassiliou (2013) concluded that a top-heavy frame is more stable than a solitary pier. This conclusion was reflected in other subsequent studies (Makris and Vassiliou, 2014; Makris and Kampas, 2016). Dar et al. (2018) showed

that the stability depends on the location of the contact point between the top beam and the pier. Hence the conclusion drawn by Makris and Vassiliou (2013) is valid for the special case shown in Figure 1(a) but not for the case in Figure 2(a), which was studied by Dar et al. (2018), where the contact points of the beam are located in between pier centers and pier corners. As shown in Figure 2(b), Dar et al. (2018) observed that $\overline{CG}$ lies above $CG$ of the pier resulting in larger size, $R_{eq}$, than that of the solitary pier, $R$, where size here is represented by the distance from the pivot point to the center of gravity of the assembly or solitary pier. However, the slenderness parameter of the assembly, represented by $\alpha_{eq}$, is lesser than the pier slenderness, $\alpha$. The location of the lumped mass, i.e., the distance of the contact point from the pier center was defined by the authors as top support eccentricity, represented by $\eta$, as shown in Figure 2(b). The authors concluded that the stability of the equivalent block is highly dependent on the combination of its size and slenderness.

Figure 2(c) shows an example rocking frame with vertically unsymmetrical piers in an NPP. Dar et al. (2019) investigated the behavior of such frames, for which the piers experience unequal rotations and the top beam does not remain horizontal. The equivalent block parameters are dependent on the instantaneous rotations of the piers and the beam, which vary with time during seismic excitation. The authors defined the polygon created by the lines joining the contact points, shown in Figure 2(a) and (c) in thick dashed grey lines, as *contact polygon*. Since sufficient friction is assumed at all contact points, there is no sliding. Hence, the side lengths of the polygon remain constant. In Figure 1(a), the distances of the contact points from their pivot points, $R_1$ and $R_1'$, being equal, means that the opposite sides of the polygon always remain parallel, and hence the piers experience equal rotations. On the contrary, in Figure 1(c), the distances of the contact points from their pivot points, $R_1$ and $R_1'$, are unequal causing the rotation angles of the two piers to be different. The authors noted that if $R_1$ and $R_1'$ are made equal by manipulating the contact point locations, even the unsymmetrical piers will experience equal rotations, and time-independent parameters of an equivalent block can be established. This paper develops expressions for these parameters and computes the seismic response of two example frames for selected earthquake records.

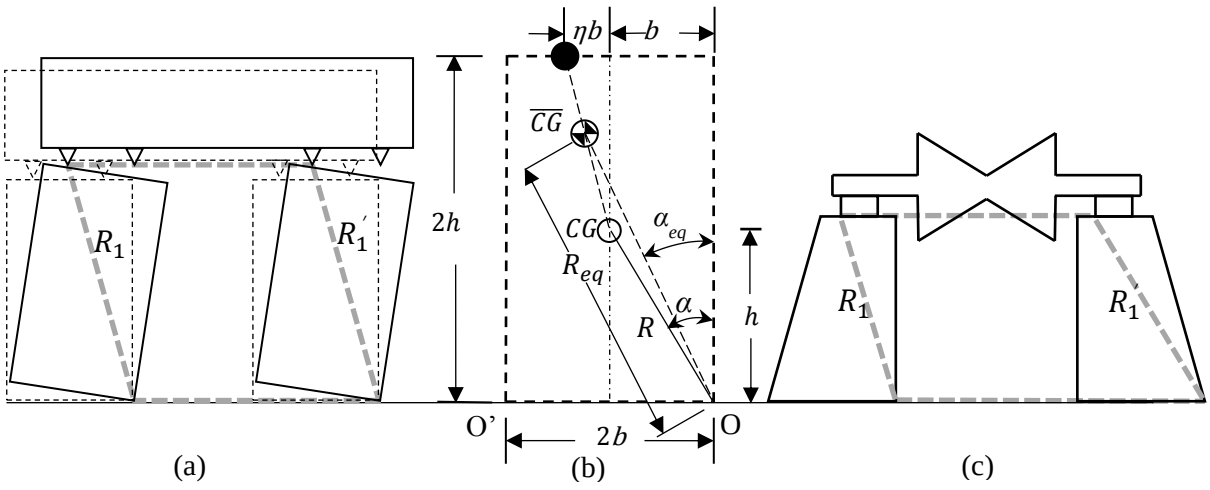


Figure 2: (a) Top beam supports in between the pier corners and pier centers, (b) pier-top-mass assembly, and, (c) schematic of a turbine rotor on unsymmetrical piers.

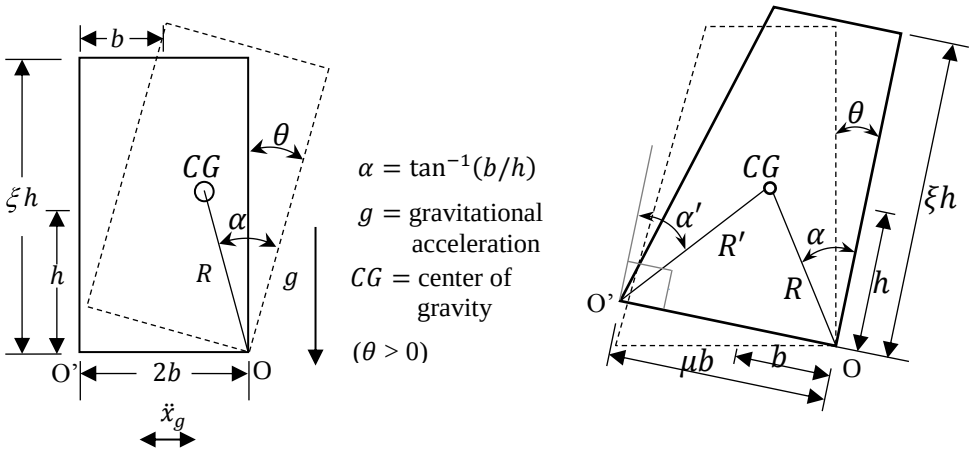


Figure 3: (a) Rectangular block, (b) unsymmetrical block

## REVIEW OF THE ROCKING BLOCK

Figure 3(a) shows the schematics of a rigid rectangular block, of mass, $m$, in rocking motion with $h$ as the height of the center of gravity ($CG$) and $b$ as the half width of the base and $I_o$ as the mass moment of inertia pivot point O. The parameter $\xi$, represents the ratio of the full-height compared to the height of the center of gravity. For a rectangular block $\xi = 2$.

For a vertically symmetrical solitary block, the equation of motion, subject to the horizontal excitation, $\ddot{x}_g$, given by Yim et al. (1980) is:

$$\ddot{\theta} = -p^2 \left\{ \sin[\alpha \, \mathrm{sgn}(\theta) - \theta] + \frac{\ddot{x}_g}{g} \cos[\alpha \, \mathrm{sgn}(\theta) - \theta] \right\} \tag{1}$$

where $g$ is the acceleration of gravity, $p = \sqrt{mgR/I_o}$ is the so-called frequency parameter, and $\mathrm{sgn}(\cdot)$ is the *signum* function. The rest of the variables are as defined above and in Figure 3. For a rectangular block, $I_o = (4/3)mR^2$ which leads to $p = \sqrt{(3g)/(4R)}$. The above equation can be solved in state-space form employing standard ODE solvers. The coefficient of restitution (Housner, 1963) accounts for the energy lost due to the impact. Multiplying the pre-impact velocity, $\dot{\theta}_1$, by the coefficient of restitution, $e$, gives the post impact velocity, $\dot{\theta}_2$. The coefficient of restitution (Housner, 1963) was revisited by Dar et al. (2018) in its generalized form for any vertically symmetrical geometry as:

$$e_G = \frac{\dot{\theta}_2}{\dot{\theta}_1} = 1 - \frac{2}{I_{on}} \sin^2 \alpha \tag{2}$$

where, $I_{on}$ is defined as the normalized moment of inertia ( $I_{on} = I_o/(mR^2)$, or $I_{on} = r_o^2/R^2$, where $r_o$ is the radius of gyration of the block about O. For a rectangular block, substituting the normalized moment of inertia, $I_{on} = 4/3$, leads to the coefficient of restitution given by Housner (1963):

$$e = 1 - \frac{3}{2} \sin^2 \alpha \tag{3}$$

Figure 3(b) shows a vertically unsymmetrical pier. Similar to Equation (1), the following equations of motion can be written for this case,

$$\ddot{\theta} = -p_p^2\left\{\sin[\alpha\ -\theta] + \frac{\ddot{x}_g}{g}\cos[\alpha\ -\theta]\right\} \text{ for } \theta > 0$$
$$\ddot{\theta} = -p_n^2\left\{\sin[-\alpha'\ -\theta] + \frac{\ddot{x}_g}{g}\cos[-\alpha'\ -\theta]\right\} \text{ for } \theta < 0 \quad (4)$$

In Equation (2), $p_p = \sqrt{mgR/I_o}$, for $\theta > 0$, and, $p_n = \sqrt{mgR'/I_{o'}}$, for $\theta < 0$, where $R'$ and $I_{o'}$ are the radius of rotation and the mass moment of inertia respectively with respect to the pivot point O'. The overturning is assumed to occur when $\theta/\alpha > 1$ for positive and $\theta/\alpha' > 1$ negative rotations respectively. The coefficients of restitution for positive and negative angular velocities as defined by Dar et al. (2019) are:

$$e_G^+ = \left(q_I - \frac{\mu(\mu-1)}{I_{on}}\sin^2\alpha\right) \text{ for } \dot{\theta} > 0$$
$$e_G^- = \frac{1}{q_I}\left(1 - \frac{\mu}{I_{on}}\sin^2\alpha\right) \text{ for } \dot{\theta} < 0 \quad (5)$$

where $\mu$ is as defined in Figure 3(b), and $q_I = I_{o'}/I_o$.

## UNSYMMETRICAL PIERS WITH EQUAL ROTATION

Figure 4(a) shows a rocking frame with unsymmetrical piers, and Figure 4(b) shows eccentricities $\eta$ and $\eta'$, chosen so as to obtain equal distances of the beam contact points from their respective pivots, $R$ and $R'$. The configuration of the rocking frame is similar to that of a turbine rotor supported on pedestals in storage in an NPP, as shown in Figure 2(c). Although each pier is unsymmetrical about the vertical axis that passes through its center of mass, they form a symmetrical rocking frame because: 1. they are mirror images of each other, and 2. their rotations are equal, owing to the particular positioning of the support points between the beam and piers. The contact polygon is shown in thick grey dashed lines.

In Figure 4(b), $R_1 = R'_1$ is achieved if $\eta + 1 = \mu - 1 + \eta'$. Dar et al. (2019) established parameters of a dynamically equivalent block for this condition which are reproduced in Table 1, where, $q_m$, is the ratio between the mass of the right pier and the mass of the left pier, considered as 1.0 in this study, and $q_T$ is the ratio of the top beam mass and the cumulative mass of the piers. The rest of the symbols have been defined in Figures 3(b) and 4(b). For calculating the response of an unsymmetrical solitary pier to seismic excitation, two sets of parameters are required to compute the response in the positive and negative directions from Equation (4). Also, two coefficients of restitution, from Equation (5), are used depending on the sign of the angular velocities at impact. For the rocking frame response, the equivalent rocking block has only one set of parameters denoted with the subscript *eq*. The equivalent block's equation of motion is the same as Equation (1) but with parameters $p_{eq}$ and $\alpha_{eq}$. Since both piers experience the same rotation, the rotation of the equivalent block would be the same as of the frame. Hence, although the piers are unsymmetrical, the frame's equivalent rocking block is symmetrical.

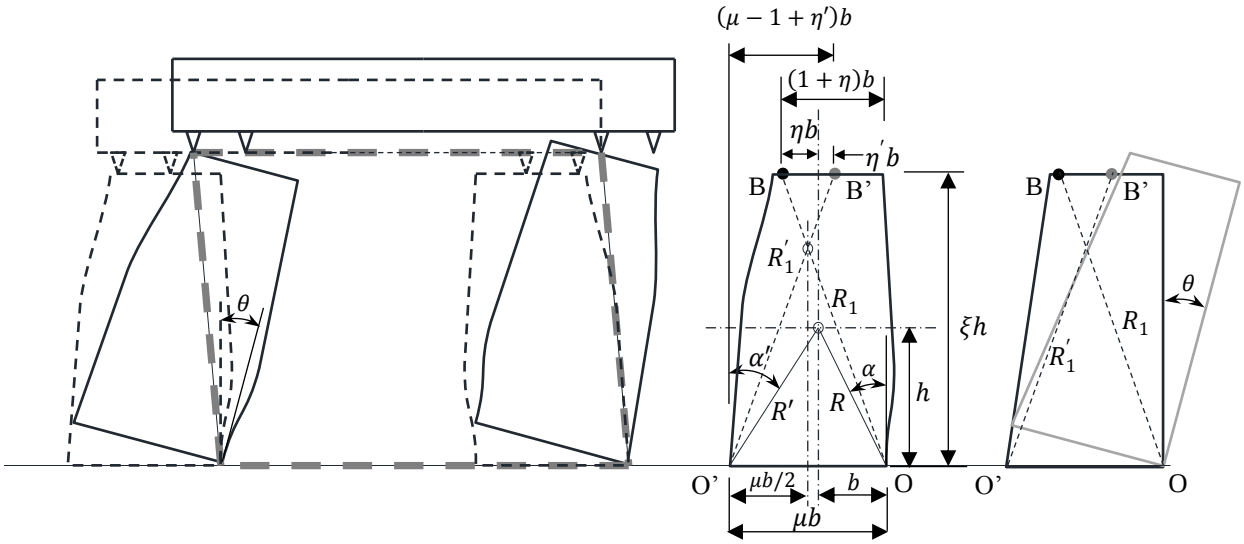


Figure 4: (a) Symmetrical rocking frame with unsymmetrical piers in rocking motion (thick grey dashed lines depict the contact polygon), (b) pier details with equal eccentricity (c) trapezoidal pier with $R_1 = R'_1$. Parameters, μ and α depend on the moment of inertia and the center of gravity of the pier geometry.

Table 1: Equivalent block parameters for a rocking frame from Dar et al (2019) and Dar et al (2018)

| | Dar et al. (2019) $\eta = \mu - 2 + \eta',\ q_m = 1$ | Dar et al. (2018) $\mu = 2,\ \eta = \eta',\ q_m = 1,\ q_T = 2q,\ q_I = 1$ |
|---|---|---|
| $\alpha_{eq}$ | $\tan^{-1}\left(\frac{1+(\mu-1)q_m+(1+\eta)q_T}{1+q_m+q_T\xi}\tan\alpha\right)$ | $\tan^{-1}\left(\frac{1+(\eta+1)q}{1+\xi q}\tan\alpha\right)$ |
| $p_{eq}^2$* | $p^2\frac{\sqrt{(1+(\mu-1)q_m+(1+\eta)q_T)^2\sin^2\alpha+(1+q_m+q_T\xi)^2\cos^2\alpha}}{1+q_I+\frac{q_T}{I_{on}}\left[(1+\eta)^2\sin^2\alpha+\xi^2\cos^2\alpha\right]}$ | $p^2\frac{\sqrt{(1+(\eta+1)q)^2\sin^2\alpha+(1+\xi q)^2\cos^2\alpha}}{1+\frac{q}{I_{on}}\left[(1+\eta)^2\sin^2\alpha+\xi^2\cos^2\alpha\right]}$ |
| $E_{eq}$ † | $\frac{e_G^+ + q_I e_G^- + \frac{q_T}{I_{on}}(\xi^2\cos^2\alpha-(1+\eta)^2\sin^2\alpha)}{1+q_I+\frac{q_T}{I_{on}}\left[(1+\eta)^2\sin^2\alpha+\xi^2\cos^2\alpha\right]}$ | $\frac{e_G+\frac{q}{I_{on}}\left[\xi^2\cos^2\alpha-(1+\eta)^2\sin^2\alpha\right]}{1+\frac{q}{I_{on}}\left[(1+\eta)^2\sin^2\alpha+\xi^2\cos^2\alpha\right]}$ |

*$I_{on} = {r_o}^2/R^2$, where, $r_o$ is the radius of gyration of the left pier about the pivot point.
†$e_G^+$ and $e_G^-$ are defined in Equation (5) and $e_G$ is in accordance with Table 2 in Dar et al. (2018)

Table 2: Rocking frame examples (for pier shape shown in Figure 4(c))

| | $\alpha$ | $\alpha'$ | $p_P$ * | $p_N$ * | $e_G^+$ | $e_G^-$ | $q_I$ | $\mu$ | $\xi$ | $\eta$ | $I_{on}$ |
|---|---|---|---|---|---|---|---|---|---|---|---|
| Example 1 | 0.49 | 0.596 | 2.249 | 2.214 | 0.63 | 0.573 | 1.1 | 2.27 | 2.1 | 0.303 | 1.36 |
| Example 2 | 0.35 | 0.434 | 1.918 | 1.902 | 0.804 | 0.764 | 1.053 | 2.27 | 2.1 | 0.303 | 1.362 |

*$p_P = \sqrt{mgR/I_o}$ and $p_N = \sqrt{mgR'/I_o}$,

Table 3: Details of Earthquake Records

| Earthquake | Year | Station | Record | PGA (g) |
|---|---|---|---|---|
| Loma Prieta, CA | 1989 | LGPC | LGP 000 | 0.563 |
| Northridge, CA | 1994 | Rinaldi | RRS 228 | 0.838 |

## RESPONSE TO EARTHQUAKE RECORDS

Table 2 shows several parameters for two examples of rocking frame piers that are required to compute the response to the earthquake records shown in Table 3. The configuration of the rocking frame is the same as shown in Figure 2(c) but with the top support locations in Figure 4(c). The response to seismic excitation is obtained by utilizing state space formulation in Mathcad (PTC, 2012) to solve Equation (4) for solitary pier response and Equation (1) for the equivalent rocking block response. At each impact, the post-impact angular velocity is updated through the coefficient of restitution value(s). Overturning is assumed to occur when the normalized rotation $\theta/\alpha_{eq} = 1$, although the literature reports occasional survival of a block with $\theta/\alpha_{eq} > 1$ (Zhang and Makris, 2001). For a solitary block, $\theta/\alpha_{eq} = \theta/\alpha$ for positive, and, $\theta/\alpha'$, for negative rotations.

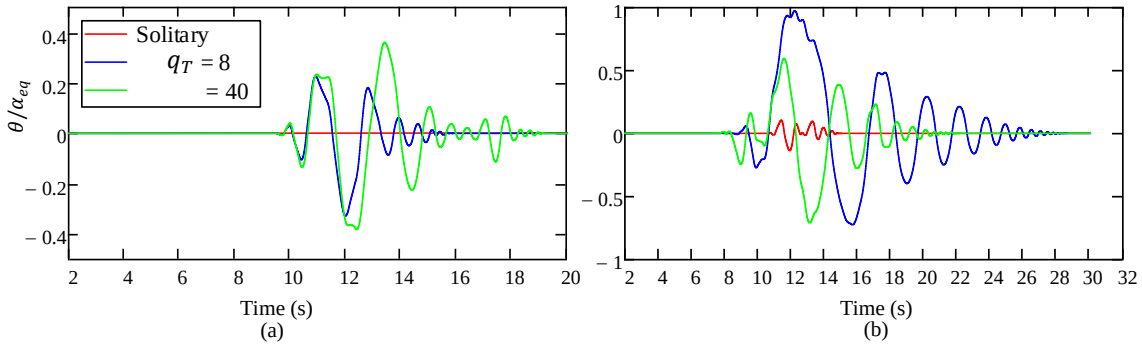


Figure 5: Response of solitary and equivalent blocks of rocking frames in Table 2 to Loma Prieta record: (a) Example 1, and (b) Example 2. For solitary block $\theta/\alpha_{eq} = \theta/\alpha$ for positive, and, $\theta/\alpha'$ for negative rotations.

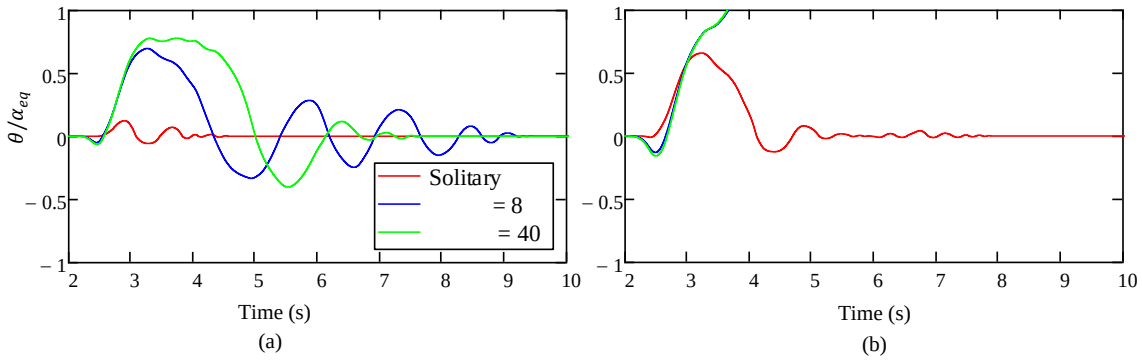


Figure 6: Response of solitary and equivalent blocks of rocking frames in Table 2 to Northridge record: (a) Example 1, and (b) Example 2.

Figure 5 shows the response of equivalent rocking blocks for piers in Example 1 and 2 in Table 2 to the Loma Prieta record given in Table 3. Three responses are shown: that of a solitary pier (no mass on top), and those of two rocking frames ($q_T = 8$ and 40). Figure 5(a) shows no response for the solitary pier, but as the beam-to-piers mass ratio $q_T$ increases, the response of the equivalent block also increases. Figure 5(b) also illustrates the same trend as Figure 5(a), but the response of the frame with $q_T = 8$ is smaller than that of the frame with $q_T = 40$.

The trend shown in Figure 6 is similar to that in Figure 5. Here also, there is a significant difference between the response of a solitary pier and that of a frame. The two figures suggest that although a stocky trapezoidal pier appears to be very stable, the addition of a beam with large mass relative to the mass of the piers appears to have a large adverse effect on stability.

## CONCLUSIONS

This paper presented a preliminary investigation on the seismic response of rocking frames with unsymmetrical piers whose top support points are strategically placed so that during an earthquake the frame's piers experience the same rotation angles, and the top beam experiences pure translation. Dynamic parameters of an equivalent block to this rocking frame configuration were presented. It was observed that the peak response of these types of frames dramatically increases with the increase in the beam-to-piers mass ratio. In two examples considered, the frame response was many times larger than the response of a solitary pier. It is concluded that heavier rocking frames with unsymmetrical piers are not necessarily more stable than their lighter counterparts.

## REFERENCES

American Society of Civil Engineers. (2005). ASCE 43-05 – Seismic Design Criteria for Structures, Systems and Components in Nuclear Facilities, Reston, Virginia, USA.

Dar, A., Konstantinidis, D., and Dakhakhni, W. W. (2018). "Seismic response of rocking frames with top support eccentricity," *Earthquake Engineering and Structural Dynamics*, (47:2496-2518).

Dar, A., Konstantinidis, D., and Dakhakhni, W. W. (2019). "Seismic response of rocking frames with top beam rotation," *Earthquake Engineering and Structural Dynamics*, (Under Review).

Dar, A., Konstantinidis, D., and El-Dakhakhni, W. (2013). "Requirement of rocking spectrum in Canadian nuclear standards," *Transactions, 22nd International Structural Mechanics in Reactor Technology Conference (SMiRT22)*. San Francisco, CA.

Dar, A., Konstantinidis, D., and El-Dakhakhni, W. W. (2015). "Seismic response of masonry rocking frames in nuclear power plants", *Transactions, 23rd International Structural Mechanics in Reactor Technology Conference (SMiRT23)*. Manchester.

Dar, A., Konstantinidis, D. and El-Dakhakhni, W. W. (2016a). "Evaluation of ASCE 43-05 seismic design criteria for rocking objects in nuclear facilities", *Journal of Structural Engineering*, 142(11), doi:10.1061/(ASCE)ST.1943-541X.0001581

Dar, A., Konstantinidis, D., and El-Dakhakhni, W. W. (2016b). "Impact of slenderness on the seismic response of rocking frames in Ontario nuclear power plants*", 5th International Structural Specialty Conference. London*, Ontario.: Canadian Society for Civil Engineering.

DeJong, M. J. and Dimitrakopoulos, E. G. (2014). "Dynamically equivalent rocking structures", *Earthquake Engineering & Structural Dynamics*, 43, 1543–1563.

Dimitrakopoulos, E. G. and Giouvanidis, A. I. (2015). "Seismic response analysis of the planar rocking frame." *Journal of Engineering Mechanics*, 141(7).

Housner, G. W. (1963). "The behavior of inverted pendulum structures during earthquakes", *Bulletin of the Seismological Society of America*, 53 (2), 403–417.

Ikushima, T. and Nakazawa, T. (1979). "A seismic analysis method for a block column gas-cooled reactor core", *Nuclear Engineering and Design*, 55, 331-342.

Konstantinidis, D. and Makris, N. (2005). "Seismic response analysis of multidrum classical columns", *Earthquake Engineering and Structural Dynamics*, 34, 1243–1270.

Kounadis, A. N., Papadopoulos, G. J., and Cotsovos, D. M. (2012). "Overturning instability of a two-rigid block system under ground excitation", *ZAMM Z. Angew. Math. Mech*., 92(7), 536 – 557.

Lee, T. H. (1975). "Nonlinear dynamic analysis of a stacked fuel column subjected to boundary motion", *Nuclear Engineering and Design*, 32, 337-350.

Makris, N. and Kampas, G. (2016). "Size Versus Slenderness: Two competing parameters in the seismic stability of free-standing rocking columns", *Bulletin of Seismological Society of America*, 106(1), 104-122.

Makris, N. and Konstantinidis, D. (2003). "The rocking spectrum and the limitations of practical design methodologies". *Earthquake Engineering and Structural Dynamics*, 32 (2), 265–289.

Makris, N. and Vassiliou, M. (2014). "Are some top-heavy structures more stable?", *Journal of Structural Engineering*, 140(5). doi:10.1061/(ASCE)ST.1943-541X.0000933, 06014001

Makris, N. and Vassiliou, M. F. (2013). "Planar rocking response and stability analysis of an array of free-standing columns capped with a freely supported rigid beam", *Earthquake Engineering and Structural Dynamics*, 42(3), 431-449.

Minafo, G., Amato, G., and Stella, L. (2016). "Rocking behaviour of multi-block columns subjected to pulse-type ground motion accelerations", *The Open Construction and Building Technology Journal*, 10(Suppl 1: M9), 150-157.

Priestley, M., Evison, R., and Carr, A. J. (1978). "Seismic response of structures free to rock on their foundations", *Bulletin of the New Zealand National Society for Earthquake Engineering*, 11(3), 141–150.

Psysharis, I. N. (1990). "Dynamic behaviour of rocking two-block assemblies", *Earthquake Engineering and Structural Dynamics*, 19, 555-575.

PTC. (2012). Mathcad 15.0. Parametric Technology Corporation, 140 Kendrick Street, Needham, MA 02494, USA.

Spanos, P. D., Roussis, P. C., and Nikolaos, P. (2001). "Dynamic analysis of stacked rigid blocks", *Soil Dynamics and Earthquake Engineering*, 21, 559-578.

Wesley, D. A., Kennedy, R. P., and Richter, P. J. (1980). "Analysis of the seismic collapse capacity of unreinforced masonry wall structures", *Proc. 7th World Conference on Earthquake Engineering*. Istanbul, Turkey.

Wittich, C. E., and Hutchinson, T. C. (2015). "Shake table tests of stiff, unattached, asymmetric structures." *Earthquake Engineering and Structural Dynamics* 44(14): 2425-43.

Wittich, C. E., and Hutchinson T. C. (2017). "Shake table tests of unattached, asymmetric, dual-body systems." *Earthquake Engineering and Structural Dynamics* 46(9): 1391–1410.

Yim, C. K., Chopra, A. and Penzien, J. (1980). "Rocking response of rigid blocks to earthquakes", *Earthquake Engineering and Structural Dynamics*, 8 (6), 565–587.

Zhang, J. and Makris, N. (2001). "Rocking response of free-standing blocks under cycloidal pulses", *Journal of Engineering Mechanics* (ASCE), 127(5), 473-483.